

Motion of the plasmoid in helical plasmas

Ryuichi ISHIZAKI¹⁾ and Noriyoshi NAKAJIMA¹⁾

¹⁾National Institute for Fusion Science, Toki 509-5292, Japan

In order to clarify the difference on the motion of a plasmoid created by a pellet injection between tokamak and helical plasmas, the MHD simulation including ablation processes has been carried out. In a straight helical plasma, the plasmoid drifts to the lower field side in several Alfvén transit times, similarly to tokamak. However, it is found that the drift direction is subsequently reversed in the case that an initial location of the plasmoid is the higher field side than one at the magnetic axis. This fact might be one of the reasons why there is the difference on the motion of the plasmoid between tokamak and helical plasmas.

Keywords: Pellet, Ablation, Drift, Tire tube force, CIP

1 Introduction

Injecting small pellets of frozen hydrogen into torus plasmas is a proven method of fueling [1]. The physical processes are divided into the following micro and macro stages. The micro stage is the ablation of mass at the pellet surface due to the high temperature bulk plasma which the pellet encounters. The neutral gas produced by the ablation is rapidly heated by electrons and ionized to form a high density and low temperature plasma, namely a plasmoid. The macro stage is the redistribution of the plasmoid by free streaming along the magnetic field lines and by MHD processes which cause mass flow across flux surfaces. The micro stage is well-understood by an analytic method [2] and numerical simulation [3]. The drift motion of the plasmoid is investigated in the macro stage [4]. Since the plasmoid drifts to the lower field side, the pellet fueling to make the plasmoid approach the core plasma has succeeded by injecting the pellet from the high field side in tokamak. On the other hand, such a good performance has not been obtained yet in the planar axis heliotron; Large Helical Device (LHD) experiments, even if a pellet has been injected from the high field side [5]. The purpose of the study is to clarify the difference on the motion of the plasmoid between tokamak and helical plasmas.

In order to investigate the motion of the plasmoid, the three dimensional MHD code including the ablation processes has been developed by extending the pellet ablation code (CAP) [3]. It is found through the comparison between simulation results and an analytical consideration that the drift motion to the lower field side in tokamak is induced by a tire tube force due to the extremely large pressure of the plasmoid and a $1/R$ force due to the magnetic pressure gradient and curvature in the major radius direction [6]. It is also found that the plasmoid does not drift when the perturbation of the plasmoid is small. In the study, the motion of the plasmoid is investigated in straight helical plasmas in the cases that the plasmoids are located

at lower and higher field sides than one at the magnetic axis. In the former case, the plasmoid drifts to the lower field side, namely to the outside. In the latter case, it drifts to the lower field side, namely to the inside at first. Subsequently, the drift direction of it is reversed, namely a part of the plasmoid drifts to the higher field side. This fact might be one of the reasons why the motion of the plasmoid does not depend on the location of the pellet injection so much in LHD experiments.

2 Basic Equations

Since the plasmoid is such a large perturbation that the linear theory can not be applied, a nonlinear simulation is required to clarify the behavior of the plasmoid. The drift motion is considered to be a MHD behavior because the drift speed obtained from experimental data [1] is about $0.01 \sim 1.0v_A$, where v_A is an Alfvén velocity. Thus, the three dimensional MHD code including the ablation processes has been developed by extending the pellet ablation code (CAP) [3]. The equations used in code are:

$$\frac{d\rho}{dt} = -\rho\nabla \cdot \mathbf{u}, \quad (1a)$$

$$\rho \frac{d\mathbf{u}}{dt} = -\frac{\beta}{2}\nabla p + (\nabla \times \mathbf{B}) \times \mathbf{B}, \quad (1b)$$

$$\frac{dp}{dt} = -\gamma p \nabla \cdot \mathbf{u} + H, \quad (1c)$$

$$\frac{\partial \mathbf{B}}{\partial t} = \nabla \times (\mathbf{u} \times \mathbf{B}) \quad (1d)$$

All variables are normalized by ones at the magnetic axis, ρ_0 , p_0 , B_0 and v_A , where $v_A = B_0 / \sqrt{\mu_0 \rho_0}$. γ and $\beta = 2\mu_0 p_0 / B_0^2$ are the ratio of the specific heats and plasma beta, respectively. Heat source H is given by:

$$H = \frac{dq_+}{dl} + \frac{dq_-}{dl}. \quad (2)$$

where q_{\pm} is the heat flux model dependent on electron density and temperature in the bulk plasma and the plas-

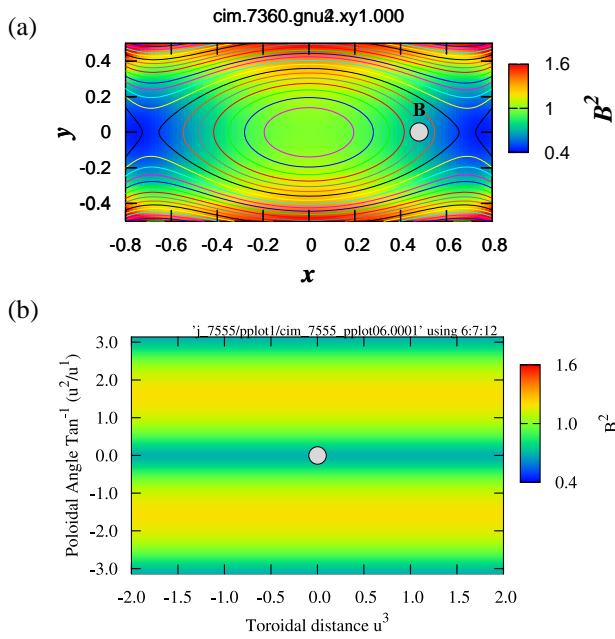


Fig. 1 Initial location of the plasmoid at lower field side than one at the magnetic axis in (a) the poloidal cross section at $u^3 = 0$ and (b) the flux surface through the center of the plasmoid in straight helical plasma. The initial location is denoted by circle. The colors show the contours of the magnetic pressures. The lines in (a) show the flux surfaces.

moid density. l is the distance along the field line. The subscript + (–) refers to the right (left)-going electrons. Then, the heat source can be calculated on each field line. Assuming Maxwellian electrons incident to the plasmoid, a kinetic treatment using a collisional stopping power formula leads to the heat flux model, q_{\pm} [3] which is used in construction of one of the ablation models [2]. The rotational helical coordinate system (u^1, u^2, u^3) is used in which the poloidal cross section (u^1 - u^2 plane) rotates along the straight toroidal direction (u^3) with same pitch as the external helical coils [7]. The Cubic Interpolated Pseudoparticle (CIP) method is used in the code as a numerical scheme [8].

3 Plasmoid simulations in straight helical

When a plasmoid is heated in tokamak plasmas, it is expanding along the magnetic field and simultaneously drifts to the lower field side due to a tire tube force and a $1/R$ force induced by the magnetic field with curvature [6]. In the study, the motion of the plasmoid is investigated in the straight helical plasma that consists of a uniform pressure and a vacuum magnetic field with $l = 2$ configuration. Figures 1(a) and (b) show the poloidal cross section (u^1 - u^2 plane) at $u^3 = 0$ and the flux surface (u^3 - θ plane) through the center of an initial plasmoid, respectively, where θ

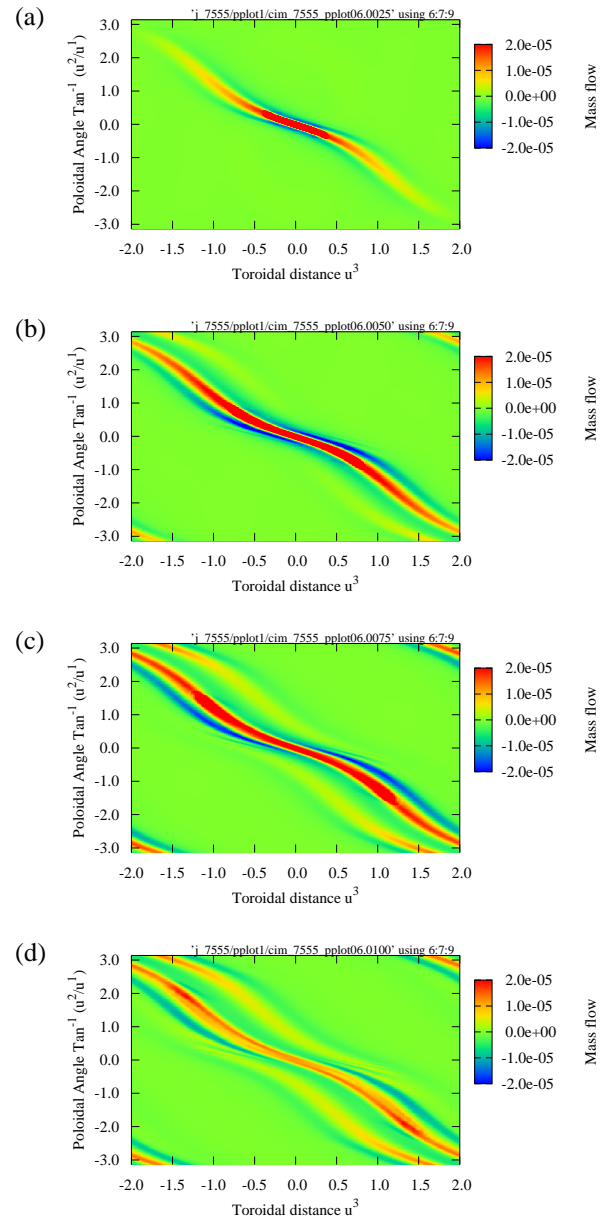


Fig. 2 Contours of the mass flow through the flux surface where the initial plasmoid is located. (a), (b), (c) and (d) are corresponding to $t = 2.5, 5.0, 7.5, 10.0 \tau_A$, respectively.

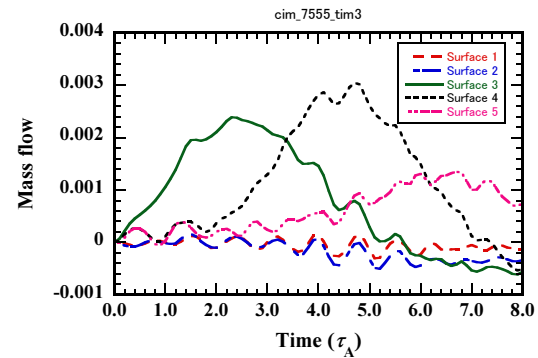


Fig. 3 Temporal evolution of mass flow integrated on the flux surfaces 1, 2, 3, 4 and 5 which are located from the magnetic axis to the outside. The initial plasmoid is located on the flux surface 3.

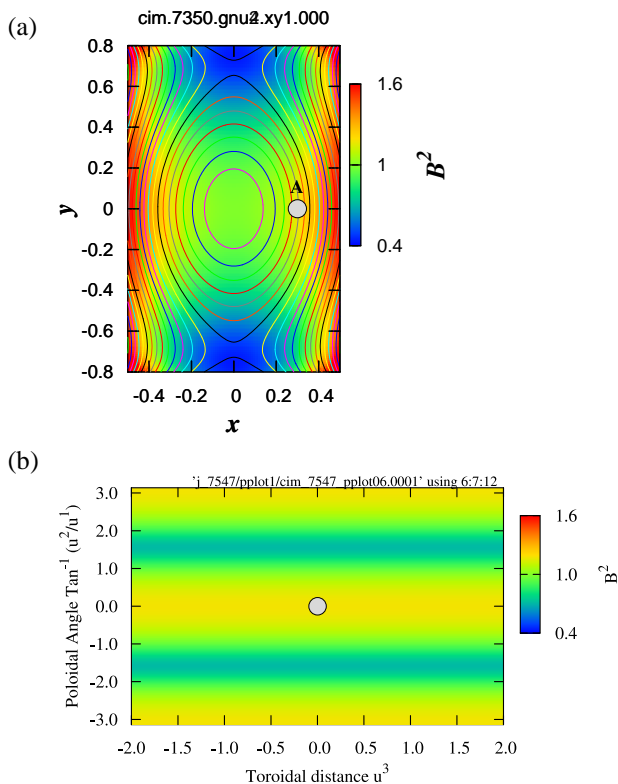


Fig. 4 Initial location of the plasmoid at higher field side one at the magnetic axis in (a) the poloidal cross section at $u^3 = 0$ and (b) the flux surface through the center of the plasmoid in straight helical plasma. The initial location is denoted by circle. The colors show the contours of the magnetic pressures. The lines in (a) show the flux surfaces.

is the poloidal angle defined by $\theta = \text{Tan}^{-1}(u^2/u^1)$. The boundaries at $u^1 = \pm 0.8$ and $u^2 = \pm 0.5$ are assumed to be the perfect conductors in Fig. 1(a). The ones at $u^3 = \pm 2.0$ are the periodic conditions in Fig. 1(b). The colors show the contours of the magnetic pressures which is uniform in u^3 -direction because the helical coordinate system is used. The lines show flux surfaces in Fig. 1(a). Initial location of the plasmoid is denoted by circle, namely it is located in the lowest field side in the flux surface. The peak values of density and temperature of the plasmoid are 100 times density and 1/100 times temperature of the bulk plasma, respectively. The plasmoid, whose half width is 0.03, encounters the electrons with fixed temperature 2 keV and density 10^{20} m^{-3} . Figure 2 shows the contours of the mass flow through the flux surface in which the initial plasmoid is located. A negative flow means one toward the magnetic axis. Figures 2(a), (b), (c) and (d) are the results at $t = 2.5, 5.0, 7.5, 10.0 \tau_A$, respectively. When the plasmoid is heated, the pressure of it increases. It is found in Fig. 2 that the plasmoid quickly expands along the magnetic field and simultaneously drifts to the outside, namely the lower field side. The fact is due to a tire tube force and a $1/R$ force induced by the magnetic field with curvature simi-

larly to the tokamak. Figure 3 shows the temporal evolution of the mass flow integrated on the flux surfaces 1, 2, 3, 4 and 5 which are located from the magnetic axis to the outside. The initial plasmoid is located on the flux surface 3. The mass flow in the surface 3 increases at first. Subsequently, it decreases after it reaches a peak value and one in the surface 4 increases because the plasmoid drifts the outside. One in the surface 5 increases after one in the surface 4 decreases. It is found that the plasmoid integrated on the flux surface also drift to the outside.

The case that the plasmoid is located at the highest field side on the flux surface is considered. Figures 4(a) and (b) show the poloidal cross section at $u^3 = 0$ and the flux surface through the center of an initial plasmoid, respectively, similarly to Figs. 1(a) and (b). The conditions except the initial location of the plasmoid are same as Fig. 1. Figures 5(a), (b), (c) and (d) show the contour of the mass flow on the flux surface at $t = 2.5, 5.0, 7.5, 10.0 \mu\text{s}$, respectively. It is found that the plasmoid quickly expands along the magnetic field and simultaneously drifts to the inside, namely the lower field side as shown in Figs. 5(a) and (b). The mass flow at $\theta = \pm\pi/2$ becomes positive as shown in Fig. 5(c) because the direction to the lower field side becomes the one to the outside. Subsequently, the mass flow at $\theta = 0$ becomes positive as shown in Fig. 5(d), namely the plasmoid drifts to the outside. In other words, it drifts to the higher field side. Figure 6 shows the temporal evolution of the mass flow integrated on the flux surfaces 1, 2, 3, 4 and 5 which are located from the magnetic axis to the outside. The initial plasmoid is located on the flux surface 3. The mass flow in the surface 3 becomes negative at first. One in the surface 2 also becomes negative because the plasmoid drifts to the magnetic axis. Subsequently, the mass flow is reversed at $\theta = \pm\pi/2$ as shown in Fig. 5(c). In addition, it is also reversed at $\theta = 0$ as shown in Fig. 5(d). The integrated mass flow is thus reversed and becomes positive. This fact might be one of the reasons why the motion of the plasmoid dose not depend on the location of the pellet injection so much in LHD experiments.

4 Summary and Discussion

It is verified by simulations using the CAP code that the plasmoid with a high pressure induced by heat flux drifts to the lower field side in spite of the initial location in an early stage for several Alfvén transit times in a straight helical plasma. Such the drift is due to a tire tube force coming from a extremely large pressure of the plasmoid and $1/R$ force of magnetic curvature similarly to tokamak. However, it is found that the drift direction is reversed in the case that an initial location of the plasmoid is the higher field side than one at the magnetic axis. This fact might be one of the reasons why there is the difference on the motion of the plasmoid between tokamak and LHD experiments. The detail analysis will be needed to clarify the physics.

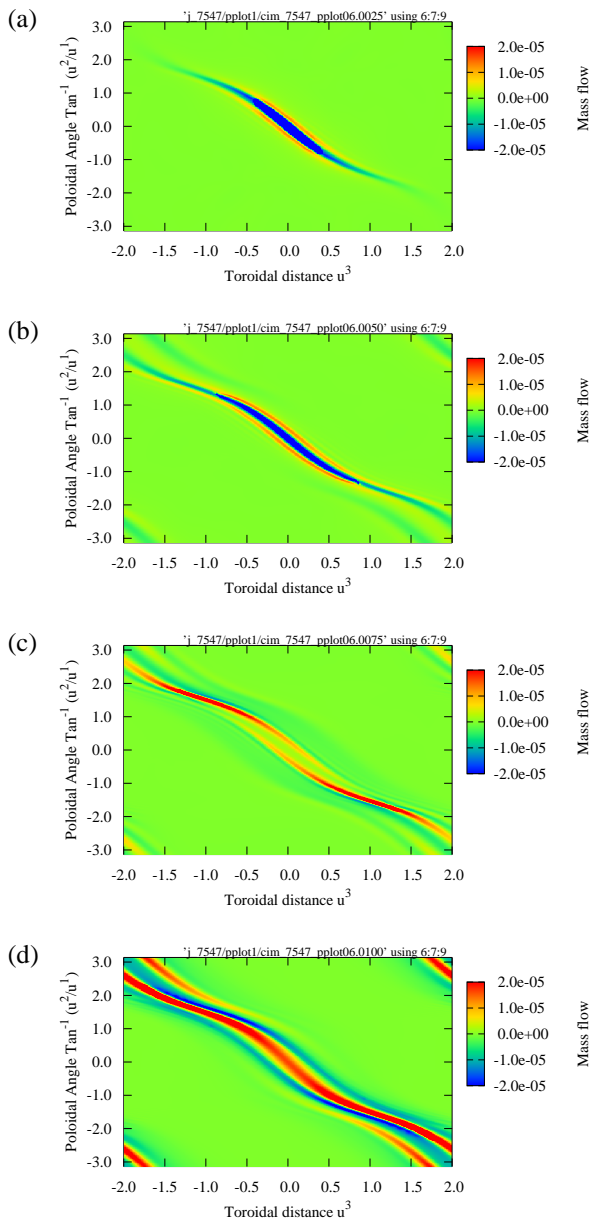


Fig. 5 Contours of the mass flow through the flux surface where the initial plasmoid is located. (a), (b), (c) and (d) are corresponding to $t = 2.5, 5.0, 7.5, 10.0 \tau_A$, respectively.

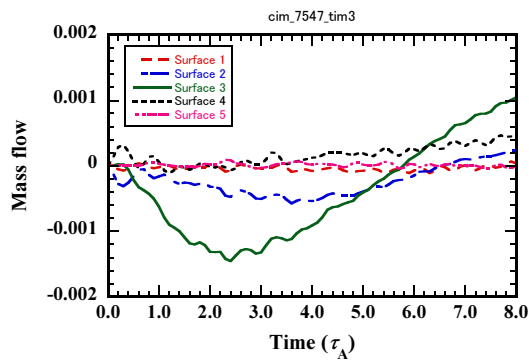


Fig. 6 Temporal evolution of mass flow integrated on the flux surfaces 1, 2, 3, 4 and 5 which are located from the magnetic axis to the outside. The initial plasmoid is located on the flux surface 3.

In addition, the simulation will be carried out in LHD configuration in order to seek the ways obtaining good performance on fueling.

- [1] Y. W. Muller et al. Nucl. Fusion, **42**, 301 (2002).
- [2] P. B. Parks and M. N. Rosenbluth. Phys. Plasmas, **5**, 1380 (1998).
- [3] R. Ishizaki et al. Phys. Plasmas, **11**, 4064 (2004).
- [4] P. B. Parks et al. Phys. Rev. Lett., **94**, 125002 (2005).
- [5] R. Sakamoto et al. in proceedings of 29th EPS conference on Plasma Phys. and Control. Fusion.
- [6] R. Ishizaki et al. IAEA-CN-149/TH/P3-6 (2006).
- [7] K. Harafuji et al. J. Comp. Phys., **81**, 169 (1989).
- [8] H. Takewaki et al. J. Comput. Phys., **61**, 261 (1985).